Supporting Information for Simultaneous dual pyrolysis synthesis of heterostructured FeCo/C porous hollow microspheres for high efficient microwave absorption

Ran Liu, [†,‡] Gaiping Du,[†,‡] Bin Liao,[†] Weixin Xiao,[†,‡] Zhenguo An,[†,], Jing-jie Zhang,[†,*]*

[†] Key Laboratory of Photochemical Conversion and Optoelectronic Materials, Technical Institute of Physics and Chemistry, Chinese Academy of Sciences, No. 29 Zhongguancun East Road, Haidian District, Beijing 100190, P. R. China;

[‡] University of Chinese Academy of Sciences, No. 19A Yuquan Road, Shijingshan District, Beijing 100049, P. R. China.

[*] To whom correspondence should be addressed. Technical Institute of Physics and Chemistry, Chinese Academy of Sciences, Beijing 100190 China. Tel/fax: +86 10 82543690.

Z.G.A. Email: zgan@mail.ipc.ac.cn.

J.-J.Z. Email: jjzhang@mail.ipc.ac.cn.

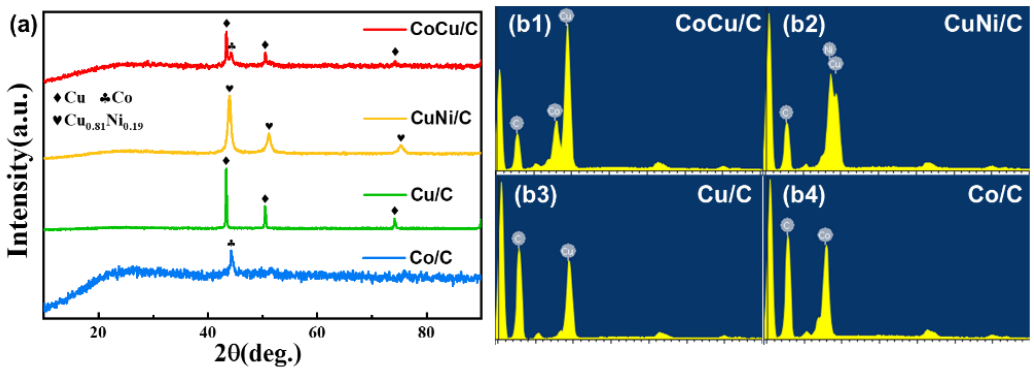

Fig. S1. (a) XRD patterns and (b) EDS analysis of carbon-metal composite hollow microspheres.

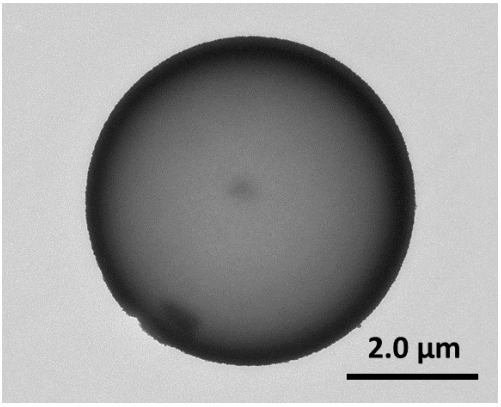

Fig. S2. Optical microscopy images of FeCo/C-2-600.

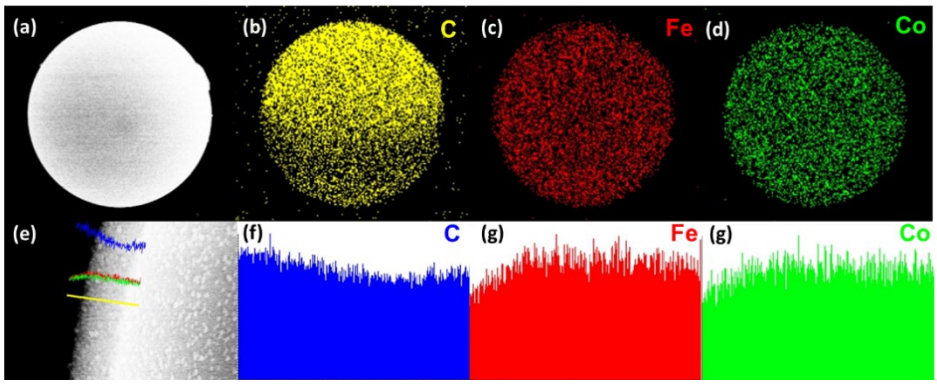

Fig. S3. (a-d) Elemental mapping on the distribution of elements for FeCo/C-2-600; (e-g) line scanning of FeCo/C-2-600.

Table S1. The tap bulk density of the FeCo-2-600

Sample	Mass (g)	Bulk volume (mL)	Tap bulk density (g/mL)
FeCo/C-2-600	0.72	3.60	0.20

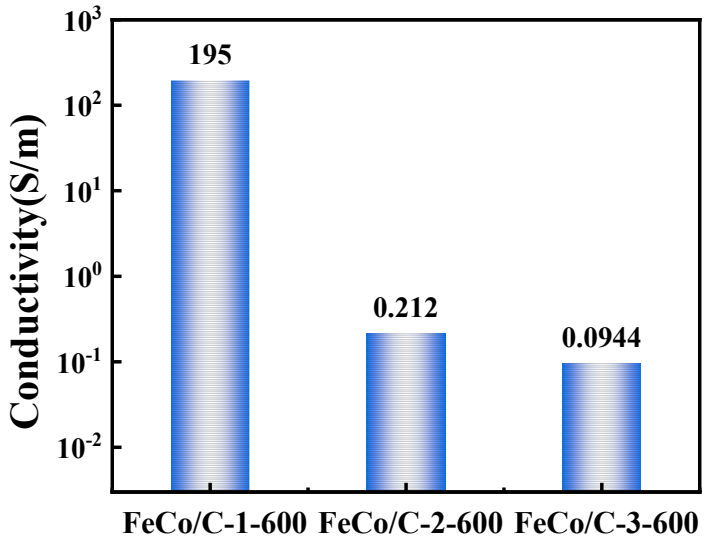

Fig. S4. Electrical conductivity of FeCo/C-X-600 (X=1,2,3).

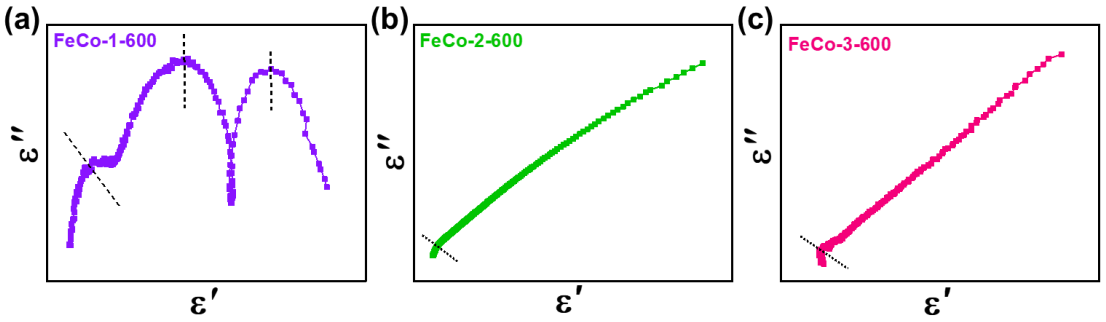

Fig. S5. Cole-Cole semicircles (ε'' versus ε') of (a)FeCo/C-1-600, (b) FeCo/C-2-600,

(c) FeCo/C-3-600.

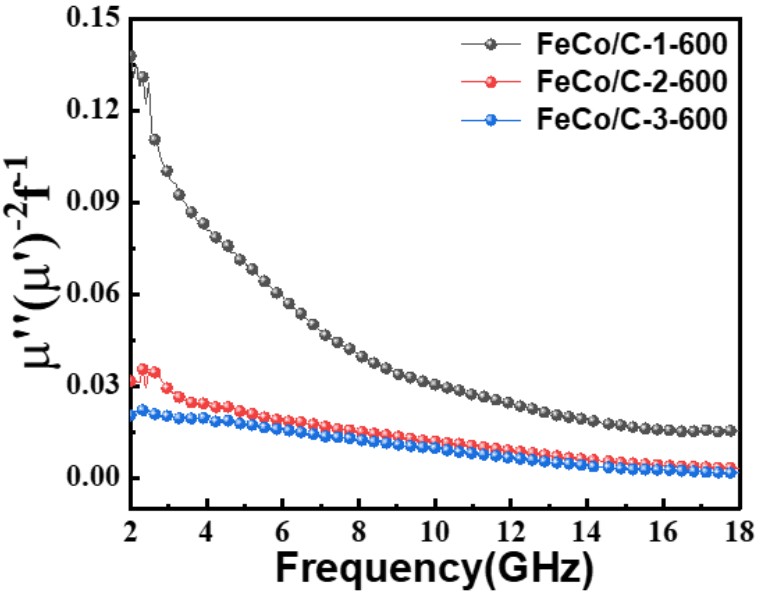

Fig. S6. Frequency dependence of of $\mu"(\mu')^{-2}f^{-1}$ for FeCo/C-X-600 (X=1,2,3).

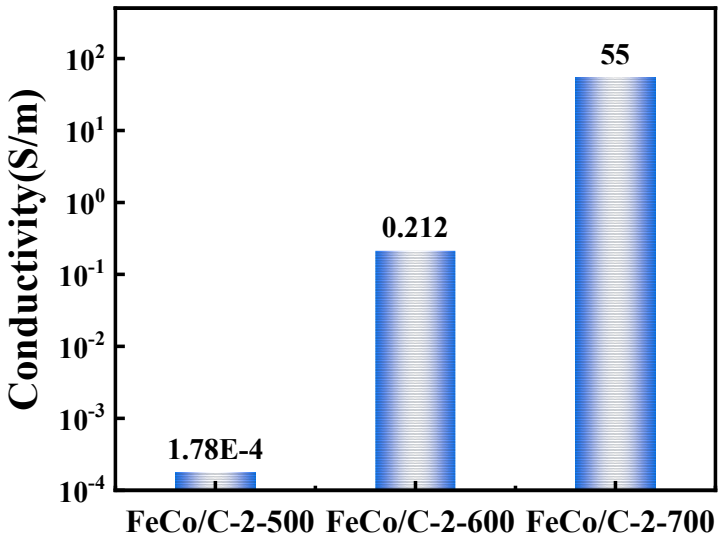

Fig. S7. Electrical conductivity of FeCo/C-2-Y (Y=500, 600, 700).

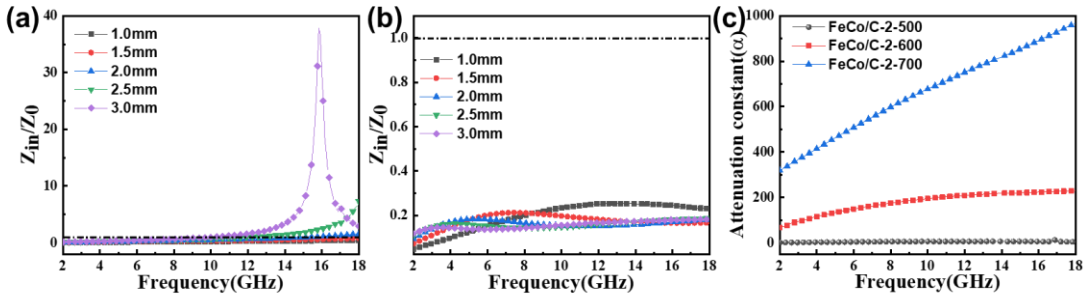

Fig. S8. Impedance matching values of (a) FeCo/C-2-500, (b) FeCo/C-2-700; (c) attenuation constant of FeCo/C-2-Y.

The impedance matching of the FeCo/C PHMs based absorbers with different temperatures is investigated to further probe the EMA mechanism of the as-obtained samples. Fig. S8(a) shows that the impedance matching of the FeCo/C-2-500 is in the range of 0.4-37.8, which is away from 1. Correspondingly, the EMA performance of the FeCo/C-2-500 is the worst (Fig. 11a). When the temperature increases to 600 °C，the impedance matching is closest to 1 (0.7-1.1, Fig. 7b), and correspondingly the absorber exhibits the best EMA performance, which is well in agreement with the results as discussed before. However, when the temperature increases to 700 °C, the impedance matching will become much lower than 1 (0.1–0.3, Fig. S8b), and correspondingly the EMA performance of the absorber will become worse (Fig. 11b). Therefore, the FeCo/C-2-600 has the best impedance matching. As shown in Fig. S8(c), among these samples, the FeCo/C-2-700 has the highest α value in almost the entire frequency range because of its high values of ε″. However, its microwave absorption performance is slightly worse than that of FeCo/C-2-600, which can be explained by the poor impedance matching characteristics. Therefore, FeCo/C-2-600 presents ultra-

strong microwave absorption performance owing to the high attenuation capacity and excellent impedance matching characteristics. From what has been discussed above, it can be inferred that proper attenuation capability and impedance matching characteristics are critical to the electromagnetic absorbing properties of the EM absorbing materials.

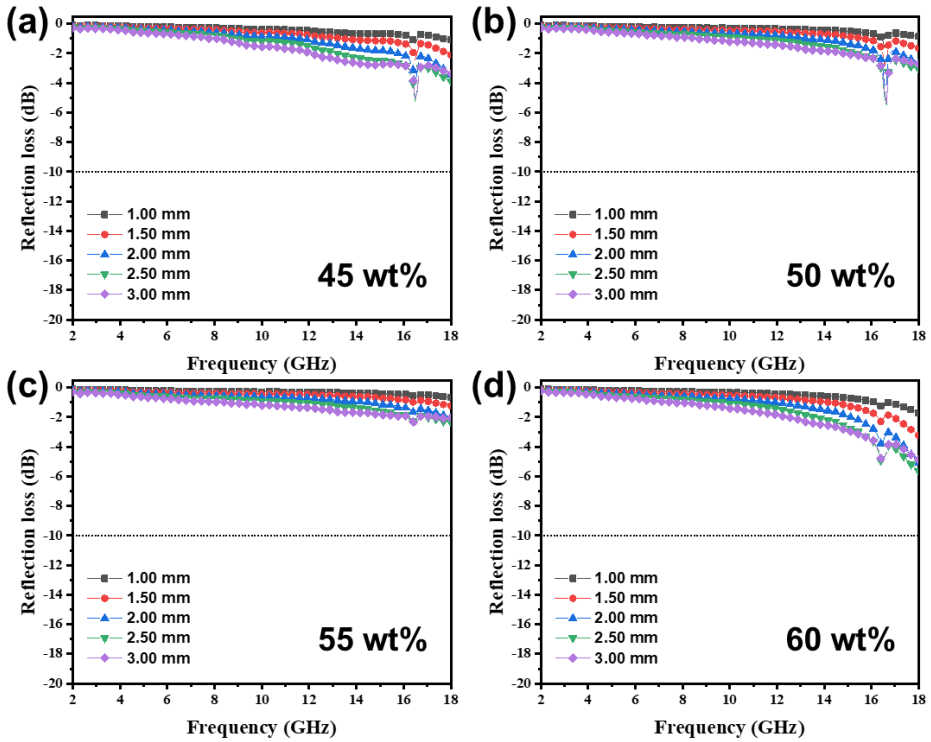

Fig. S9. The 2D RL curves of the sample (a) FeCo/C-2-500-45, (b) FeCo/C-2-500-50, (c) FeCo/C-2-500-55, (d) FeCo/C-2-500-60.